

# Naval Research Laboratory

Stennis Space Center, MS 39529-5004



NRL/MR/7176--96-7717

## **The Effects of Variable Time Window Width and Signal Position Within FFT Bin on WISPR Performance**

JACOB GEORGE  
RONALD A. WAGSTAFF

*Ocean Acoustics Branch  
Acoustics Division*

February 9, 1996

19960305 097

Approved for public release; distribution unlimited.

DTIC QUALITY INSPECTED 1

# ROUTINE REPLY, ENDORSEMENT, TRANSMITTAL OR INFORMATION SHEET

OPNAV 5216/158 (Rev. 7-78)  
SN 0107-LF-052-1691

A WINDOW ENVELOPE MAY BE USED  
Formerly NAVEXOS 3789

CLASSIFICATION (UNCLASSIFIED when detached from enclosures, unless otherwise indicated)

UNCLASSIFIED

FROM (Show telephone number in addition to address) DSN 485-4739 COMM 601-688-4739

DATE

27 FEB 1996

DIRECTOR

NAVAL RESEARCH LABORATORY STENNIS, SSC, MS, 39529-5004

SERIAL OR FILE NO.

7032.2/07-96

SUBJECT

SUBMISSION OF DOCUMENTS TO DTIC FOR ON-LINE CATALOGING

REFERENCE

ENCLOSURE

TO:

DEFENSE LOGISTICS AGENCY  
DEFENSE TECHNICAL INFORMATION CENTER  
8725 JOHN J. KINGMAN ROAD, SUITE 0944  
FT. BELVOIR, VA 22060-6218

NRL/MR/7176--96-7717  
NRL/MR/7323--96-7722  
NRL/MR/7322--95-7684  
NRL/FR/7174--95-9623

VIA:

ENDORSEMENT ON

☒ FORWARDED ☐ RETURNED ☐ FOLLOW-UP, OR TRACER ☐ REQUEST ☐ SUBMIT ☐ CERTIFY ☐ MAIL ☐ FILE

GENERAL ADMINISTRATION		CONTRACT ADMINISTRATION		PERSONNEL	
FOR APPROPRIATE ACTION		NAME & LOCATION OF SUPPLIER OF SUBJECT ITEMS		REPORTED TO THIS COMMAND:	
UNDER YOUR COGNIZANCE		SUBCONTRACT NO. OF SUBJECT ITEM			
INFORMATION		APPROPRIATION SYMBOL, SUBHEAD, AND CHARGEABLE ACTIVITY		DETACHED FROM THIS COMMAND	
APPROVAL RECOMMENDED <input type="checkbox"/> YES <input type="checkbox"/> NO		SHIPPING AT GOVERNMENT EXPENSE <input type="checkbox"/> YES <input type="checkbox"/> NO		OTHER	
<input type="checkbox"/> APPROVED <input type="checkbox"/> DISAPPROVED		A CERTIFICATE, VICE BILL OF LADING			
COMMENT AND/OR CONCURRENCE		COPIES OF CHANGE ORDERS, AMENDMENT OR MODIFICATION			
CONCUR		CHANGE NOTICE TO SUPPLIER			
LOANED, RETURN BY:		STATUS OF MATERIAL ON PURCHASE DOCUMENT			
SIGN RECEIPT & RETURN					
REPLY TO THE ABOVE BY:					
REFERENCE NOT RECEIVED		REMARKS (Continue on reverse)			
SUBJECT DOCUMENT FORWARDED TO:		NRL/FR/7174--95-9623 Volume Reverberation on CST III			
SUBJECT DOCUMENT RETURNED FOR:		NRL/MR/7322--95-7684 Variations of Ice Cover and Thermohaline Structure in the Arctic -GIN Sea Basin...			
SUBJECT DOCUMENT HAS BEEN REQUESTED, AND WILL BE FORWARDED WHEN RECEIVED		NRL/MR/7323--96-7722 Warfighting Contributions of the Geosat Follow-on Altimeter			
COPY OF THIS CORRESPONDENCE WITH YOUR REPLY		NRL/MR/7176--96-7717 The Effects of Variable Time Window Width and Signal Position Within FFT Bin on WISPR Performance			
ENCLOSURE NOT RECEIVED					
ENCLOSURE FORWARDED AS REQUESTED					
ENCLOSURE RETURNED FOR CORRECTION AS INDICATED					
CORRECTED ENCLOSURE AS REQUESTED					
REMOVE FROM DISTRIBUTION LIST					
REDUCE DISTRIBUTION AMOUNT TO:					
SIGNATURE & TITLE		Linda H. Jenkins HEAD, CLASSIFIED LIBRARY			

COPY TO:

7032.2L

CLASSIFICATION (UNCLASSIFIED when detached from enclosures, unless otherwise indicated)

REPORT DOCUMENTATION PAGE			Form Approved OBM No. 0704-0188	
Public reporting burden for this collection of information is estimated to average 1 hour per response, including the time for reviewing instructions, searching existing data sources, gathering and maintaining the data needed, and completing and reviewing the collection of information. Send comments regarding this burden or any other aspect of this collection of information, including suggestions for reducing this burden, to Washington Headquarters Services, Directorate for Information Operations and Reports, 1215 Jefferson Davis Highway, Suite 1204, Arlington, VA 22202-4302, and to the Office of Management and Budget, Paperwork Reduction Project (0704-0188), Washington, DC 20503.				
1. AGENCY USE ONLY (Leave blank)		2. REPORT DATE February 9, 1996		3. REPORT TYPE AND DATES COVERED Final
4. TITLE AND SUBTITLE  The Effects of Variable Time Window Width and Signal Position Within FFT Bin on WISPR Performance			5. FUNDING NUMBERS  Job Order No. 571683006 Program Element No. 0602435N Project No. Task No. VW35202 Accession No.	
6. AUTHOR(S) Jacob George and Ronald A. Wagstaff				
7. PERFORMING ORGANIZATION NAME(S) AND ADDRESS(ES) Naval Research Laboratory Center for Environmental Acoustics Stennis Space Center, MS 39529-5004			8. PERFORMING ORGANIZATION REPORT NUMBER  NRL/MR/7176--96-7717	
9. SPONSORING/MONITORING AGENCY NAME(S) AND ADDRESS(ES) Office of Naval Research 800 N. Quincy Street Arlington, VA 22217-5000			10. SPONSORING/MONITORING AGENCY REPORT NUMBER	
11. SUPPLEMENTARY NOTES				
12a. DISTRIBUTION/AVAILABILITY STATEMENT  Approved for public release; distribution unlimited			12b. DISTRIBUTION CODE	
13. ABSTRACT (Maximum 200 words)  The effect of variable width of the time window in time-frequency analysis on WISPR performance is investigated, along with the effect of signal position within the signal bin. The results demonstrate that variable width of the time window in FFT/DFT calculations has only a small effect on WISPR performance, as long as the full signal energy is contained within the signal bin. But the loss of even a small portion of the signal energy from the signal bin has a dramatic effect on the WISPR level, and causes deterioration in WISPR performance by several decibels. The average power level is only slightly affected by such changes. The sensitivity of the WISPR level to the signal position within the signal bin provides a means to determine the signal frequency more precisely, avoiding the necessity to carry out calculations using much larger data sets.				
14. SUBJECT TERMS  fluctuations, noise, WISPR processing			15. NUMBER OF PAGES 17	
			16. PRICE CODE	
17. SECURITY CLASSIFICATION OF REPORT Unclassified	18. SECURITY CLASSIFICATION OF THIS PAGE Unclassified	19. SECURITY CLASSIFICATION OF ABSTRACT Unclassified	20. LIMITATION OF ABSTRACT SAR	

# The effects of variable time window width and signal position within FFT bin on WISPR performance

Jacob George and Ronald A. Wagstaff

NRL Ocean Acoustics Branch, Code 7176, Stennis Space Center, MS. 39529

## 1. Introduction

Fluctuations are always present in underwater sound propagation, and are generally viewed as a complication in the signal identification and extraction process. However, in some important cases where the signals fluctuate less than the noise, it is possible to exploit the different natures of the signal and noise fluctuations to achieve a greater signal-to-noise ratio (S/N). Wagstaff's Integration Silencing Processor (WISPR) [1-4] is one example of a non-linear processor which takes advantage of the relatively larger fluctuations of the noise compared to those of the steadier signal, to provide S/N gains and other enhancements. The WISPR processing technique has been successfully applied to several experimental situations.

The complex pressures / power values which form the data set from which average WISPR levels and average power levels are calculated, are typically obtained from Fourier transforms of hydrophone output voltage time series. Usually the time series values in the finite window are multiplied by a window function such as Gaussian or Hann. Such a transform has been called a "short-time Fourier transform" (STFT) [5]. For example, the Gabor transform which has a Gaussian window function can be written as

$$S(f, \tau) = \int_{-\infty}^{+\infty} dt \cdot s(t) \cdot \exp\left[-\frac{1}{2}\left(\frac{t-\tau}{\sigma}\right)^2\right] \cdot \exp(i2\pi ft) \quad (1)$$

While the width of the time series window in the STFT is independent of frequency ( $\sigma$  in Eq. (1)

being a constant), other transforms in which this width vary inversely proportional to frequency have been proposed and are being studied extensively [5]. For example, the Morlet transform can be written as [6]

$$S(f, \tau) = \sqrt{f} \int_{-\infty}^{+\infty} dt \cdot s(t) \cdot \exp \left[ -\frac{1}{2} \left( \frac{t-\tau}{\xi/f} \right)^2 \right] \cdot \exp (i 2\pi f t), \quad (2)$$

where  $\xi$  is a constant. This latter kind of transforms have been applied to time-frequency analyses to produce improved resolution [7, 8]. This is illustrated in Fig. 1, which compares the results of time-frequency analyses using the STFT and the Morlet transforms [7]. In the example of Fig. 1, the Morlet transform produces improved resolution compared to the STFT.

Since WISPR processing involves the calculation of several types of averages of complex pressure / power values over periods of time, the improved resolutions due to wavelet transforms such as those in Refs. 7 and 8 could possibly improve WISPR performance. In such applications of wavelet transforms to WISPR processing, the frequency dependence of the width of the time window would be an important factor. The variable width can affect WISPR performance in two ways:

(a) A smaller time window entails a larger frequency bin width, greater noise in the signal bin, and consequently a possible deterioration in WISPR performance.

(b) Even if the signal width in frequency space is less than the FFT / DFT bin width, varying the time window width can cause a portion of the signal energy to fall in a bin adjacent to the main signal bin. The effect of this on WISPR performance needs to be investigated.

A discussion of these factors is the subject of the present report. The investigation has been conducted using the example of a successful application of the WISPR processor in the detection of a submerged source. That example is briefly described in Section 2. The effect of varying the width of the time window is discussed in Section 3. The sensitivity of the WISPR processor to the position of the signal within its FFT / DFT frequency bin is discussed in Section 3.

## 2. WISPR Example

The example of a successful application of the WISPR processor in the detection of a submerged source is described in the present section, along with the relevant theoretical details. This example will be used in the investigations described below. The version of the WISPR processor used here is one that includes phase variations [4]. In order to briefly describe this processor, consider the complex pressures for a given frequency bin calculated by an FFT from a time series of hydrophone voltages. These complex pressures, which also form a time series, may be either the output from a single hydrophone, or the beamformed output from an array of hydrophones. Let the set  $\{z_n\}$  ( $n = 1, 2, \dots, N$ ) denote the complex pressures from a single hydrophone or from a single beam. The  $n^{\text{th}}$  complex pressure is of the form

$$z_n = r_n u_n \quad (3)$$

where  $r_n$  is the magnitude, and  $u_n$  is the complex phase factor. This phase factor is of the form

$$u_n = \exp \{i[\theta_n + 2\pi f(t + n\Delta t)]\} \quad (4)$$

where  $f$  is the frequency, and  $\Delta t$  is the time delay between the successive FFTs. The phase factors corresponding to the time delay  $\Delta t$  can be removed from the set  $\{u_n\}$ , yielding a new set  $\{v_n\}$  as

$$v_n = u_n \exp(-i2\pi f n \Delta t) = \exp[i(\theta_n + 2\pi f t)] \quad (5)$$

The average of the set  $\{v_n\}$  is given by

$$\bar{s} = \frac{1}{N} \sum_{n=1}^N v_n \quad (6)$$

Now defining a quantity  $R$  as

$$R = \left[ \frac{1}{N} \sum_{n=1}^N r_n^{-1} \right]^{-1}, \quad (7)$$

the WISPR value is taken to be

$$W = (R \cdot |\bar{s}|)^2 \quad (8)$$

The corresponding average WISPR level in decibels is then

$$W_{dB} = 10 \log W. \quad (9)$$

The conventional definition of the average power for the set  $\{z_n\}$  is

$$P = \frac{1}{N} \sum_{n=1}^N |z_n|^2, \quad (10)$$

and the corresponding average power level in decibel is

$$P_{dB} = 10 \log P. \quad (11)$$

Having defined the WISPR level (including phase fluctuations) in Eq. (9), it is now straightforward to calculate the function  $(P_{dB} - W_{dB})$ . For a beam containing a steady tonal such as that from a submerged source, the WISPR level  $W_{dB}$  would be nearly equal to the power level  $P_{dB}$ , and therefore the function  $(P_{dB} - W_{dB})$  would be nearly zero [1-4]. In contrast, the function  $(P_{dB} - W_{dB})$  would have a relatively large positive value for a noise beam [1-4].

The above concepts are illustrated in Fig. 2, showing results from a Pacific experiment which employed a 144 element hydrophone horizontal line array. The beampattern for the signal in the frequency bin 5.225 - 5.322 Hz is shown in Fig. 2 (sampling rate: 200 Hz; FFT size: 2048 points; time series overlap between successive FFTs: 75%, Hann window). The WISPR level is approximately 15 dB lower than the average power level on all beams except in the vicinity of beam number 118, which indicates a steady submerged source by a sudden dip in the difference function  $(P_{dB} - W_{dB})$ . It is important to point out that the average power level plot (the top curve) does not indicate such an unambiguous detection, because it exhibits an even larger peak in the vicinity of beam number 139, produced by a strong but fluctuating surface source.

### 3. Variable Time Window Width

The effect of varying the width of the time window was studied by repeating the above calculation using different numbers of DFT points in the initial extraction of amplitudes from the time series. As in Fig. 2, all calculations reported below focus on the signal in the vicinity of 5.25 Hz, and use the Hann window. In Fig. 3, the difference function ( $P_{dB} - W_{dB}$ ) is plotted along the Y-axis, and the plots show the effect of decreasing the number of DFT size from 2048 points to 948 points, and to 722 points. In all three cases the signal bin fully contained the signal. (The importance of this point will become clear by the discussions in Section 4). As the DFT size decreases, the width of the signal bin correspondingly increase from 0.097 Hz to 0.211 Hz, and to 0.259 Hz, allowing in more noise and causing more fluctuations. As a consequence, the goodness of detection deteriorated, but only slightly, as indicated by the decreasing dip in the vicinity of beam number 118. This change is rather small, since the difference function ( $P_{dB} - W_{dB}$ ) at beam number 118 changes from approximately 2 dB (for 2048 DFT points) to approximately 5 dB (for 722 DFT points), in comparison with higher values (approximately 15 dB) for noise beams.

### 4. Signal Position Within FFT Bin

The WISPR level has been observed to be very sensitive to the position of the signal within the FFT / DFT frequency bin. In order to demonstrate this, we start with Fig. 4 which shows the average power level of the signal in the vicinity of 5.25 Hz plotted vs. frequency, obtained from 16000 point DFTs. The calculation of Fig. 2 was repeated with DFT sizes 1964, 1966, 1968, ....., 1994, 1996. Figure 5 shows the upper edges and the lower edges (in frequency space) of the signal bin in each case, with the plus signs indicating the points at which the DFT calculations were made. The signal shape of Fig. 4 is marked to scale on the right hand side of Fig. 5. The dashed lines in Fig. 5 represent the optimum window location as judged from Fig. 7 below.

The average power level  $P_{dB}$ , the standard deviation  $\sigma$  of the power levels, and the WISPR level  $W_{dB}$  are plotted in Fig. 6 as functions of frequency for DFT sizes 1964, 1966, 1968, ....., 1994, 1996. Each frequency value is the median frequency of the signal bin for the corresponding DFT. The signal shape from Fig. 4 is also shown. The signal bin width is approximately 0.10 Hz for all the DFTs, and is shown labeled "window size". The average power level  $P_{dB}$ , the standard deviation  $\sigma$  of the power levels, the WISPR level  $W_{dB}$ , and the difference function ( $P_{dB} - W_{dB}$ ) are shown in greater detail in Fig. 7. The point at approximately 5.295 Hz corresponds to the 1964 point DFT, and the point at approximately 5.21 Hz corresponds to the 1996 point DFT. An examination of the signal shape and the signal bin width in Fig. 6 reveals that for the

1964 point DFT (5.295 Hz) and for the 1996 point DFT (5.21 Hz), small portions of the signal energy lie outside the signal bin. In spite of this, the average power levels at these points differ only less than 1 dB from their peak value which occurs at approximately 5.25 Hz (Fig. 7). However, the WISPR level is significantly affected, and it changes by as much as 5 dB from its peak level (Fig. 7). Since the smallness of the difference function is the criterion for detection of stable signal sources, it is clear that WISPR detection capability deteriorates when even a small portion of the signal energy falls outside the signal bin, as at 5.295 Hz and at 5.21 Hz.

The above observations are confirmed by the results in Figure 8(a), which shows the upper edges and the lower edges of the signal bin for DFT sizes 948, 972, 986, and 1024. The dashed lines represent the optimum window location as judged from Fig. 7. Clearly portions of the signal energy for the 972 point DFT falls outside the signal bin for this case. Figure 8(b) shows that the corresponding WISPR level is about 14 dB lower than the other WISPR levels where the complete signal energy falls within the signal bin. In contrast, this variation has only a miniscule effect on the average power.

## 5. Conclusions

The foregoing analysis demonstrates that variable width of the time series window in FFT / DFT calculations has only a small effect on WISPR performance, provided that the full signal energy is contained within the signal bin. When the signal position within the signal bin is such that a small portion of the signal energy falls outside the signal bin, the average power level is only slightly affected. However, such loss of even a small portion of the signal energy from the signal bin has a dramatic effect on the WISPR level, and causes deterioration in WISPR performance by several decibels. Therefore, in applications of wavelet transforms to WISPR processing, special care must be taken to ensure that the signal bin contains the full signal energy, and that no portion of this energy falls in adjacent bins.

The most effective ways to do WISPR processing accurately when the signal energy necessarily has to fall in at least two or more frequency bins due to small bin width, is a topic that remains to be investigated.

The sensitivity of the WISPR level to the signal position within the signal bin can be used to determine the signal frequency more precisely, avoiding the necessity to carry out calculations using much larger data sets.

## 6. Acknowledgments

This work was performed under the Program Element number PE0602435N, and was supported by the Office of Naval Research, Mr. Tommy Goldsberry, Program Manager.

## References

- [1] R. A. Wagstaff, "The WISPR filter: A method for exploiting fluctuations to achieve improved sonar signal processor performance," (submitted to J. Acoust. Soc. Am.)
- [2] J. George and R. A. Wagstaff, "Variations of WISPR levels and average power levels with standard deviation," NRL Memorandum Report No. NRL/MR/7176--93-7077 (1994).
- [3] J. George and R. A. Wagstaff, "WISPR performance measured by ROC curves," NRL Memorandum Report No. NRL/MR/7176--94-7559 (1994).
- [4] R. A. Wagstaff and J. George, "A new fluctuation based processor including phase variations", (to be submitted to J. Acoust. Soc. Am.)
- [5] C. K. Chui, *An Introduction to Wavelets*, (Academic, New York, 1992), Ch. 3.
- [6] H. H. Szu, B. Telfer, and A. Lohmann, "Causal analytical wavelet transform", *Optical Eng.* 31, 1825 (1992)
- [7] M. Badiy, I. Jaya, and A. H. D. Cheng, "Shallow water acoustic/geoacoustic experiments at the New Jersey Atlantic generating station site," *J. Acoust. Soc. Am.* **96**, 3593-3604 (1994).
- [8] D. M. Drumheller, et.al., "Identification and synthesis of acoustic scattering components via the wavelet transform," *J. Acoust. Soc. Am.* **97**, 3649-3656 (1995).

## Figure Captions

Figure 1. Comparison of the results of time-frequency analyses using (a) the "short-time Fourier transform", and (b) the Morlet transform (from Ref. 7).

Figure 2. The beampattern for the signal (including noise) in the frequency bin 5.225 - 5.322 Hz from a Pacific experiment employing a 144 hydrophone horizontal line array (sampling rate: 200 Hz; FFT size: 2048 points; Hann window). The average power level, the WISPR level, and the difference between the two are labeled.

Figure 3. The effect of varying the size of time window on WISPR performance. The difference function ( $P_{dB} - W_{dB}$ ) is plotted along the Y-axis.

Figure 4. The average power level of the signal in the vicinity of 5.25 Hz plotted vs. frequency, obtained from 16000 point DFTs.

Figure 5. The upper edges and the lower edges of the signal bin for DFT sizes 1964, 1966, 1968, .... , 1994, 1996. The plus signs indicate the points at which the DFT calculations were made. The dashed lines represent the optimum window location as judged from Fig. 7.

Figure 6. The average power level  $P_{dB}$ , the standard deviation  $\sigma$  of the power levels, and the WISPR level  $W_{dB}$  plotted as functions of frequency for DFT sizes 1964, 1966, 1968, .... , 1994, 1996. Each frequency value is the median frequency of the signal bin for the corresponding DFT. The plus signs indicate the points at which the DFT calculations were made.

Figure 7. The average power level  $P_{dB}$ , the standard deviation  $\sigma$  of the power levels, the WISPR level  $W_{dB}$ , and the difference function ( $P_{dB} - W_{dB}$ ) plotted as functions of frequency for DFT sizes 1964, 1966, 1968, .... , 1994, 1996. Each frequency value is the median frequency of the signal bin for the corresponding DFT. The plus signs indicate the points at which the DFT calculations were made.

Figure 8(a): The upper edges and the lower edges of the signal bin for DFT sizes 948, 972, 986, and 1024. The plus signs indicate the points at which the DFT calculations were made. The dashed lines represent the optimum window location as judged from Fig. 7. Fig. 8(b): The average power level  $P_{dB}$ , the standard deviation  $\sigma$  of the power levels, and the WISPR level  $W_{dB}$ , for DFT sizes 948, 972, 986, and 1024.

Figure 1

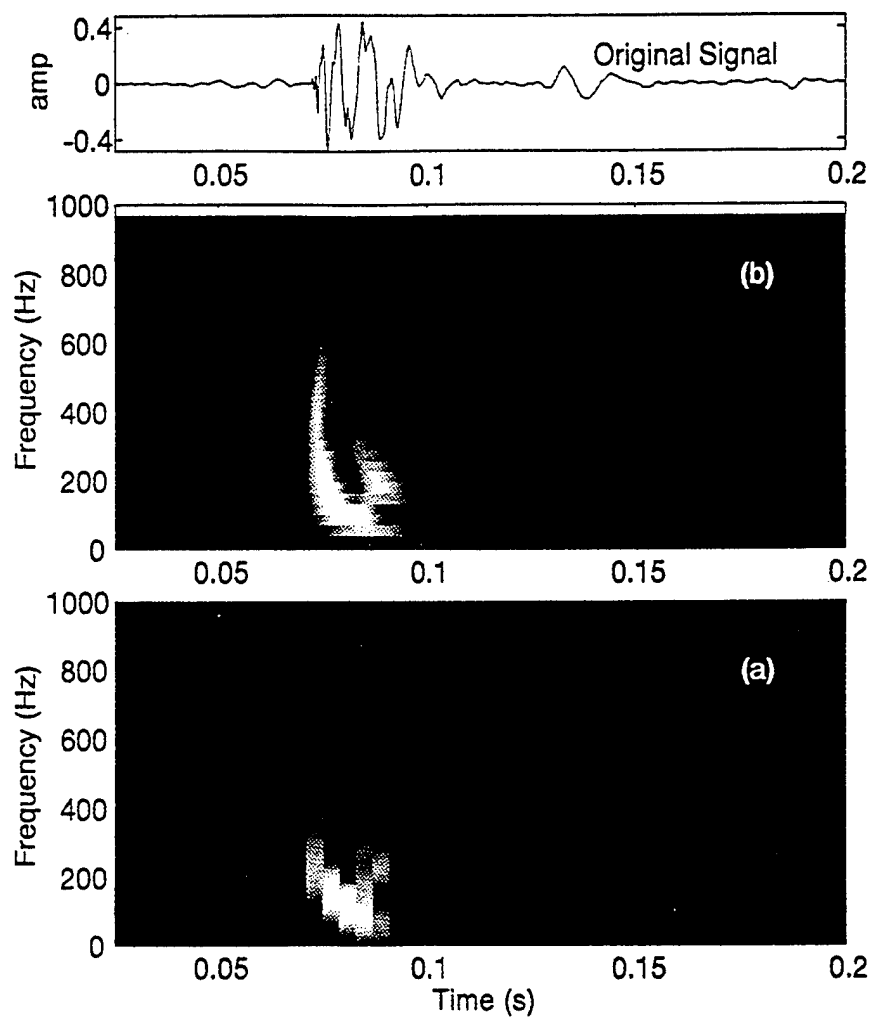


Figure 2

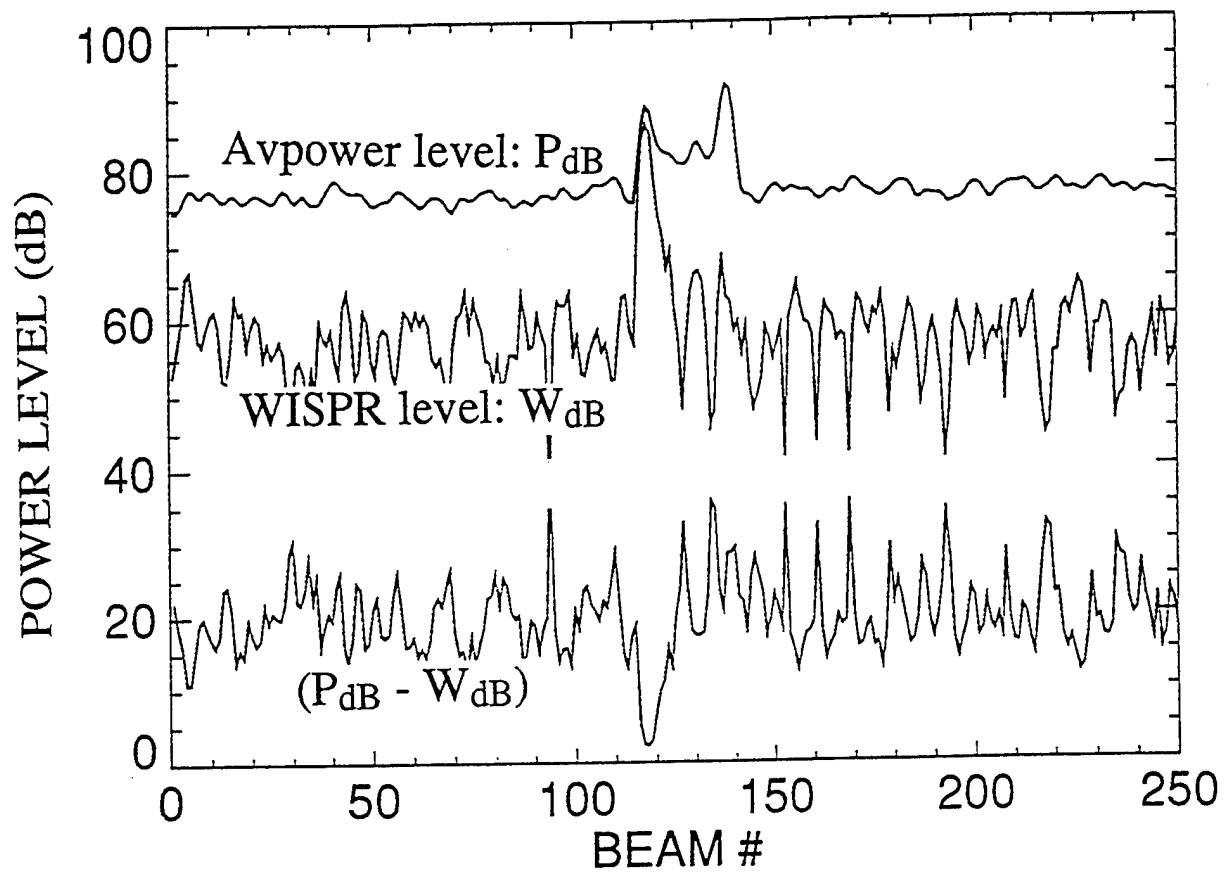


Figure 3

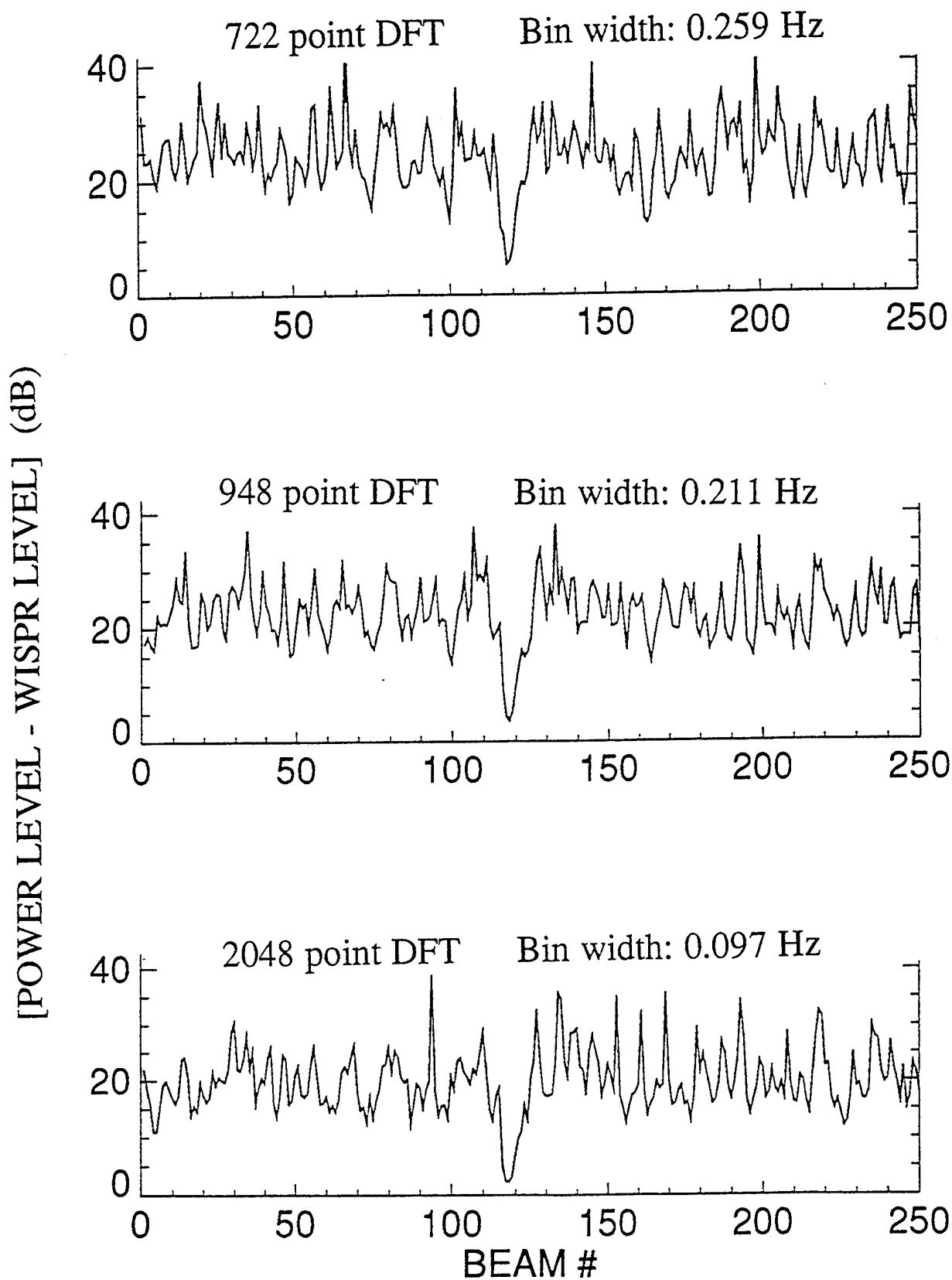


Figure 4

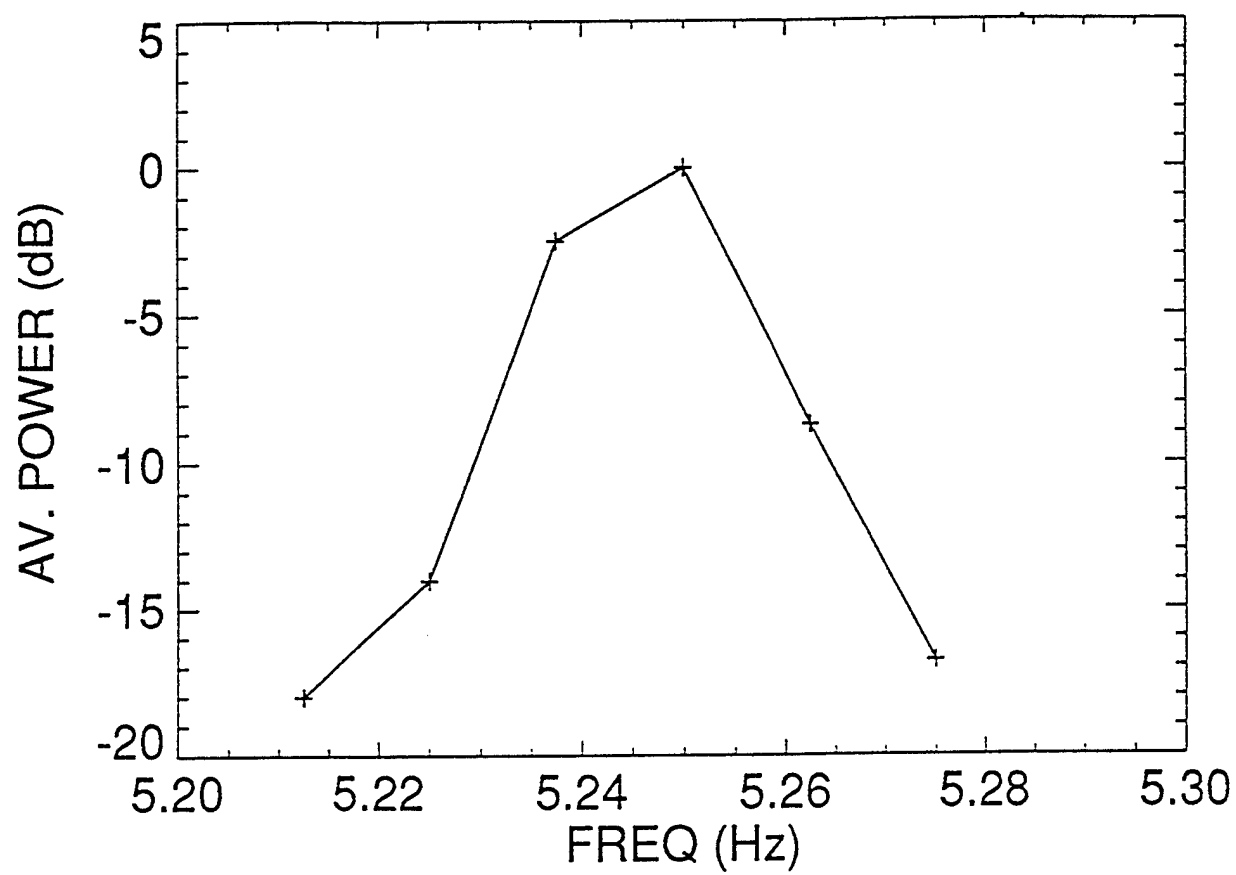


Figure 5

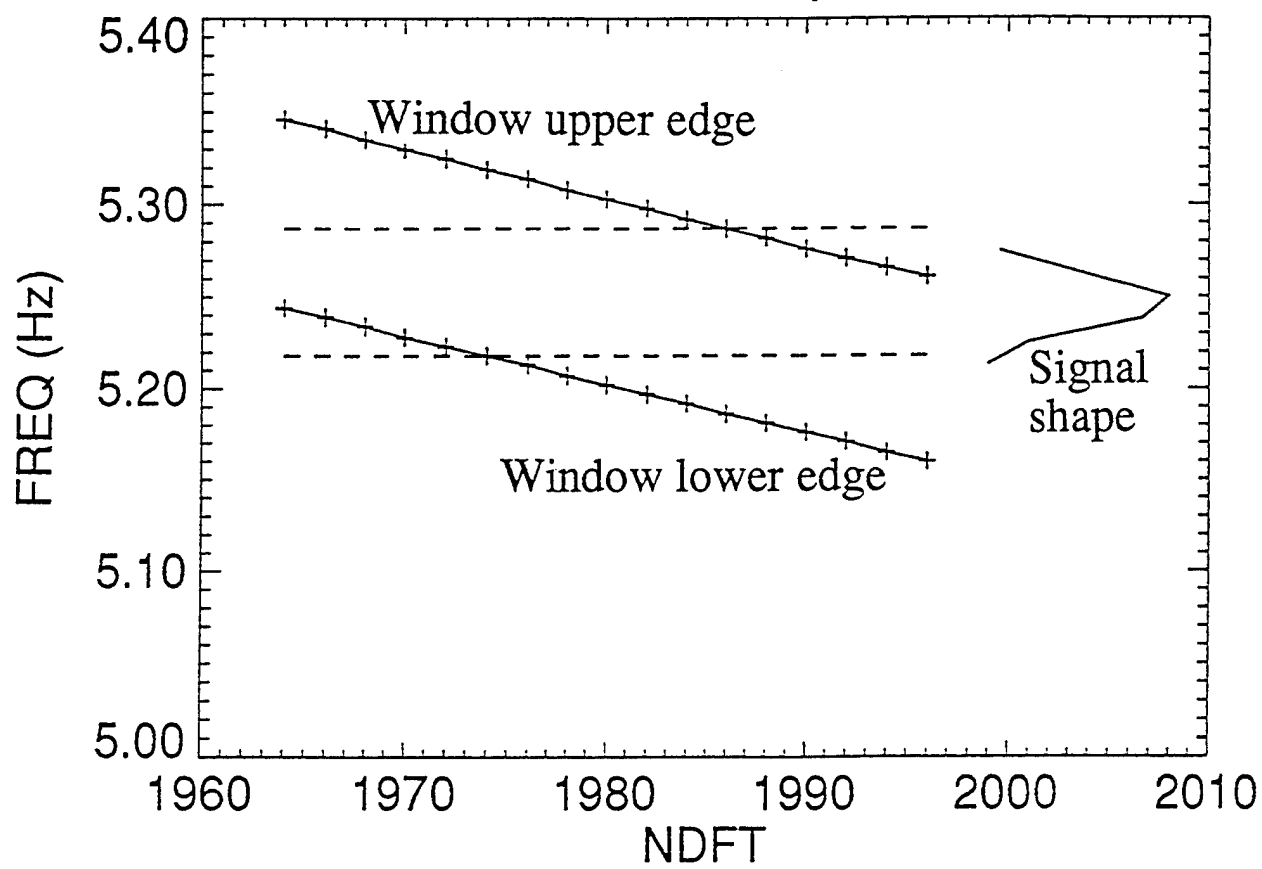


Figure 6

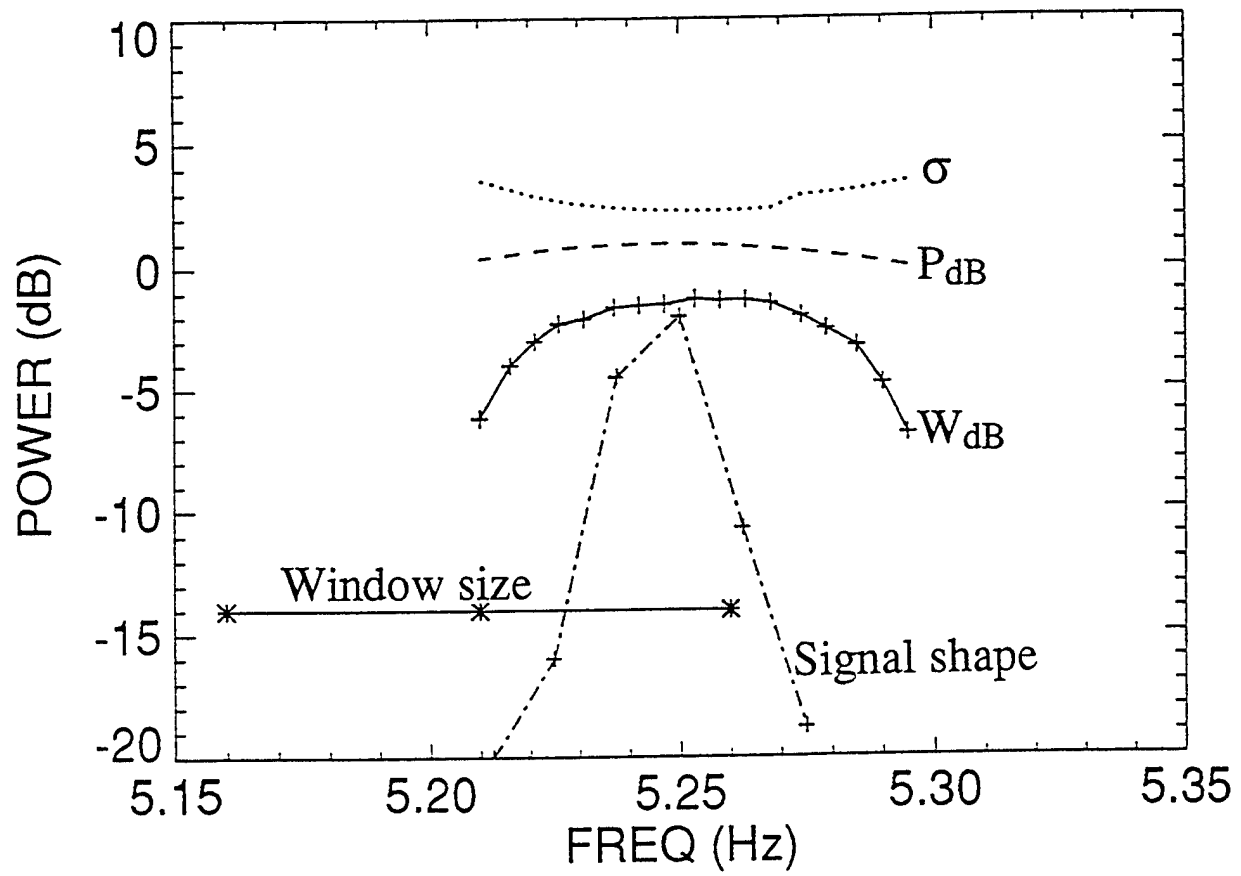


Figure 7

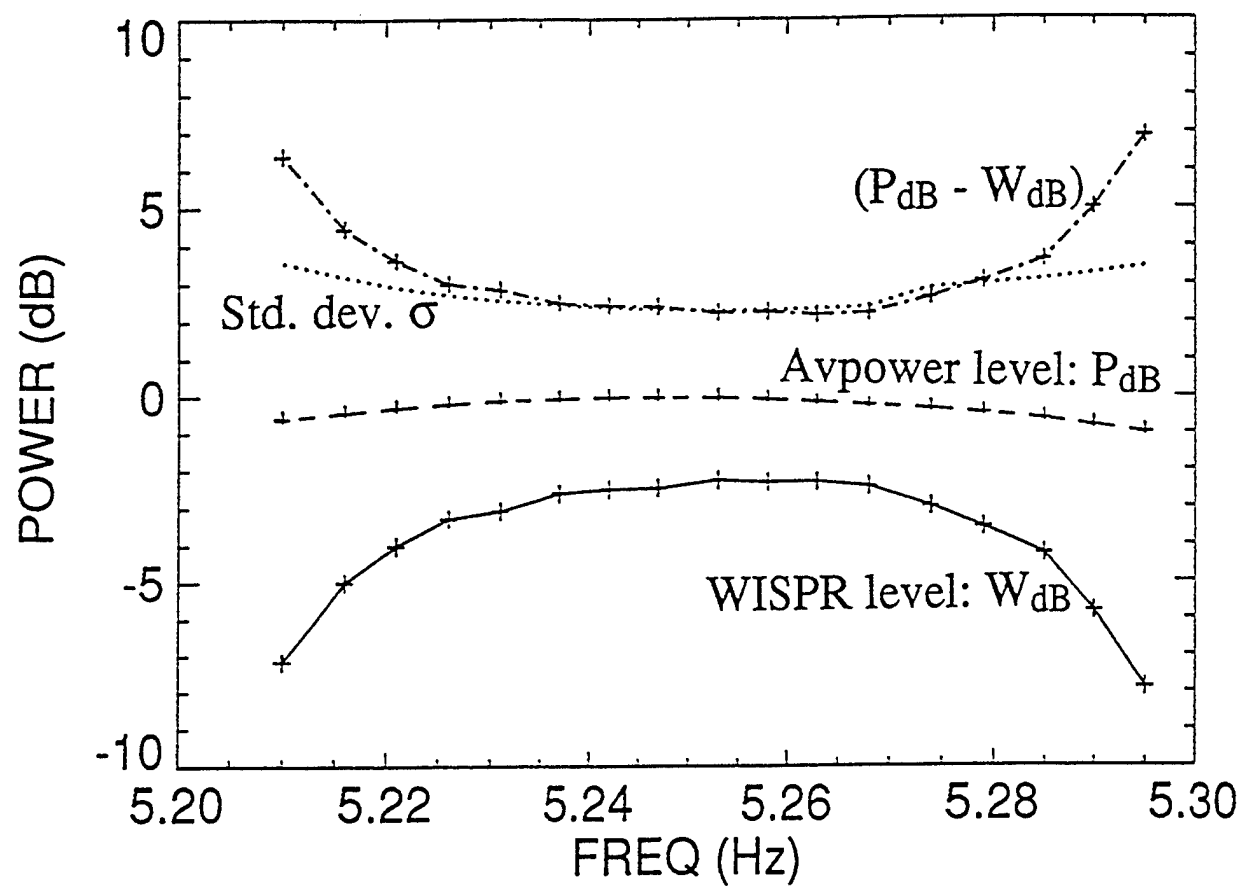


Figure 8

